Microwave-Assisted Synthesis and Characterization of Novel $Ru_xM_{1-x}Al_2O_3$ Nanoparticles

Hüseyin Köksal[1]*, Othman Abdulrahman Hamad[2]

[1]Kahramanmaraş Sütçü İmam University, Faculty of Science and Arts, Chemistry Department, Kahramanmaraş, Turkey

[2]Raparin University, Faculty of Science, Chemistry Department, Raniya, Iraq

ABSTRACT: In this study, three metal composed of nanostructures of $Ru_xM_{1-x}Al_2O_3$ have been successfully synthesized by a simple and rapid microwave-assisted method using thiourea as the fuel and ethylene glycol (EG) as the reducing agent. In comparison with conventional heating, microwave-assisted method shortens the reaction time. The morphology, particle size and microstructure were analyzed using SEM and XRD. Microwave irradiation has yielded nanosized spherical phase particles. The mean grain size of the nanoparticles less than 100 nm. The FT-IR studies confirms the presence of metal–oxygen and metal-oxygen-metal bond. XRD and SEM of the synthesized nanoparticles show that the prepared nano compounds have low crystallinity and sphere and flower-like shape. Flower shape $Ru_{0.63}Co_{0.37}Al_2O_3$, $Ru_{0.93}Ni_{0.07}Al_2O_3$ and $Ru_{0.54}Cu_{0.46}Al_2O_3$ particles were obtained. Generally, the crystallite sizes were found in the range of 41-94 nm. The EDX analysis indicated that the elements of Ru, Fe, Co, Ni, Cu and Al existed in the products. The surface treatment of spray gold for elimination of charged effects were responsible for the signals of gold in the EDX analysis of the products. In other words, no impurities like N, S, P, Cl, etc. were detected except for Ru, Fe, Co, Ni, Cu and Al elements, indicating the nanoparticles were pure.

Keywords: *Nanoparticles, microwave-assisted, metal oxide*

Yeni $Ru_xM_{1-x}Al_2O_3$ Nano Parçacıkların Mikrodalga Destekli Sentezi ve Tanımlanması

ÖZET: Bu çalışmada, yapısında üç metal bulunan nanoyapılar basit ve hızlı mikrodalga-yardımlı metod ile sentezlenmiştir. Bu sentezlerde tiyoüre yakıt olarak kullanılırken, etilen glikol (EG) yüzey gerilimini düşürücü ve indirgen olarak kullanılmıştır. Bilinen eski yöntemlerle kıyaslandığında bu yöntem reaksiyon süresini kısaltmıştır. Oksitlerin morfolojisi, parça büyüklüğü ve mikroyapısı SEM ve XRD ile analiz edilmiştir. Mikrodalga radyasyonu nanobüyüklükte küresel fazlı parçacıklar üretmiştir. Nanoparçacıkların ortalama tanecik boyutu 100 nm'den küçüktür. FT-IR çalışmaları metal-oksijen ve metal-oksijen-metal bağlarının varlığını doğrulamaktadır. Sentezlenen nanopartiküllerin XRD ve SEM sonuçları nano bileşiklerin düşük kristaliniteye sahip olduğunu, küresel ve çiçek-benzer şekillerde olduğunu göstermektedir. Çiçek tipi $Ru_{0.63}Co_{0.37}Al_2O_3$, $Ru_{0.93}Ni_{0.07}Al_2O_3$ ve $Ru_{0.54}Cu_{0.46}Al_2O_3$ parçacıkları elde edilmiştir. Genelde, kristal büyüklükleri 41-94 nm aralığındadır. EDX analizleri sentezlenen bileşiklerin yapısında Ru, Fe, Co, Ni, Cu ve Al elementlerinin varlığını doğrulamaktadır. Bileşiklerin EDX analizlerinde gözlemlenen Altın elementine ait pik, yük etkisini yok etmek amacıyla yüzeye püskürtülen Altın'a aittir. Ek olarak, yapılarda N, S, P ve Cl gibi safsızlıkların olmayışı ve yalnız Ru, Fe, Co, Ni, Cu ve Al elementlerin gözlemlenmesi, nanoparçacıkların saf olduğunu göstermektedir.

Anahtar Kelimeler: *Nanoparçacıklar, mikrodalga-destekli, metal oksit*

1. INTRODUCTION

The metal oxides materials have found numerous applications, such as gas sensors, UV photodiodes, piezoelectric devices, varistors, acoustic wave devices, transparent electrodes, facial powders and some metal oxides, an n-type, II–IV semiconductor, are commercially important materials used in solar cells, rubber, sensors, varistors, etc. Recently, a wide range of research on synthesizing metal oxides with one dimensional nanostructures such as nanorods, fibers, tubes, wires, ribbons, nano needle sand nano sheets have gained much importance due to their potential applications in various fields. These nanostructured materials have been prepared by many methods such as microwave heating; non-aqueous approaches; chemical-precipitation; sol-gel process; gas condensation;

hydrothermal process; aerosol spray process ; and hydrolysis in polyol medium [1, 2].

Microwave heating methods can avoid the problem of heating inhomogeneity. In fact, it has been demonstrated that microwave irradiation can enhance reaction rates, selectivity, and product yields, which owes to the efficient transformation of energy and the homogeneity of temperature distribution in the reaction vessel [3]. As we know, the properties and applications of nanomaterials depend not only on their composition, but also on their structure, shape and size distribution. Thus, morphology-controlled synthesis of nanomaterials with well-defined shapes is an important goal in the field of modern nanomaterials. Nanoparticles (NPs), because of their small size, have high surface area to volume ratios which affects their individual properties as well as their interparticle interactions. This large surface area and the changed electronic properties are very important for applications of NPs in several areas of science and industry, especially in catalysis due to their high activity [4–7]. Ru is an important member of the group of platinum metals, cheaper than Pd or Pt, and its nanoparticles (Ru NPs) show very unique and interesting activities as a catalyst [8]. For example, they can act as major catalysts in the hydrogenation reaction of monoaromatics [9], methanol fuel cells [10], synthesis of diesel fuels [11], and removal of organic pollutants from water [12], etc. Out of many methods used for the synthesis of NPs, the use of microwave dielectric heating has been shown to dramatically reduce processing times, increase product yields, and enhance product purity compared to many other processes [13]. Microwave chemistry, produces rapid internal heating by direct interaction of electromagnetic irradiation with the molecules, i.e., solvents, reagents and catalysts, which are present in the reaction mixture [14]. The application of microwave irradiation reduces metal ions to produce NPs of different shapes and sizes. An advantage for precise tuning is that experimental parameters like irradiation power, reaction temperature and pressure inside the vessel can be controlled precisely in microwave synthesis. The reducing and stabilizing agents used are glucose and polyethyleneglycol (PEG) which are biodegradable in nature. [15]

2. MATERIALS

Analytical grade compounds used in experiments were purchased from Merck, Fluka and Sigma-Aldrich and used without further purification. An appropriate ratio of metal salts thiourea to serve as fuel and precipitating agent in synthesis reactions. Among the known fuels, thiourea and urea seems to be the most convenient fuel to be employed, given that it is cheap and readily available commercially as well as its employment is safer in comparison with carcinogenic hydrazine-based hydrazide fuels. The ethylene glychol (EG) agent used for chemical precipitation can interact with ions through ethylene oxygen groups (-CH2CH2O-) in the molecules and mediate the size and morphology nanoparticles. At the same time, EG can enwrap the precipitations and reduce the aggregation among the NPs. In addition, EG have large exclusion volume in aqueous solutions, and thus can provide additional strict hindrance among the NPs, which can also inhibit particle aggregation. Chemical precipitation with MW-assisted method is simple easily to produce high yield and hence rapid reaction occurs. EG also acts as a reducing agent to reduce the metal ion to metal oxide [27]..

3. EXPERIMENTAL

3.1. Preparation of $Ru_{0.4}Fe_{0.6}Al_2O_3$ NPs

In a typical experimental procedure, The $Ru_{0.4}Fe_{0.6}Al_2O_3$ NPs were prepared from a mixture including (0.4 mmol, 0.105g) of $RuCl_3.3H_2O$, (0.7 mmol, 0.283g) of $Fe(NO_3)_3.9H_2O$, (2 mmol, 0.649 g) of Aluminum acetylacetonate ($Al(C_5H_7O_2)_3$), each substance dissolved in small amount of deionized water with vigorous stirring in microwave teflon container tube (50 ml) and then thiourea (1 mmol, 0.076 g) was added to metal solution mixture and dissolved in addition of 10 ml deionized water to form a black-blue solution. At the end tube was filled with 10 ml of ethylene glycol (EG) and closed with teflon closer. The obtained mixture was located at the center of a microwave system and irradiated in constant power (600 W). The exposure time was 60 min at 200 °C. After the reaction was terminated, the product was allowed to cool to room temperature, the resulting dark black powders were rinsed and washed with deionized water and absolute ethanol several time until free from impurities. The precipitate was dried at 75 °C in a vacuum oven for 10 h to get the sample of $Ru_{0.4}Fe_{0.6}Al_2O_3$. The $Ru_{0.4}Fe_{0.6}Al_2O_3$ nanoparticle has been characterized with the SEM, EDX, XRD analyses and FT-IR technique. The FT-IR, SEM, EDX and XRD of NPs are shown in Fig.1, 2, 3 and 4, respectively.

3.1.1. Preparation of $Ru_xM_{1-x}Al_2O_3$ NPs (M:Co, Ni, Cu) NPs

Spherical RuxM1-xAl2O3 architectures were prepared by a microwave-assisted process. In a typical experimental procedure, RuxM1-xAl2O3 was prepared from a mixture including (0.4 mmol 0.105g) of RuCl3.3H2O, (0.6 mmol) of M (II) chloride, (2 mmol, 0.267g) of Aluminum chloride (AlCl3), each substance dissolved in small amount of deionized water with vigorous stirring in microwave teflon container tube (50 ml) and then (1 mmol, 0.076 g) thiourea was added to metal solution mixture and dissolved in addition of 10 ml deionized water to form a black-blue solution. At the end tube was filled with 10 ml of EG and closed with teflon closer. The obtained mixture was located at the center of a microwave system and irradiated in constant power

(600 W). The exposure time was 60 min at 200 °C. After the reaction was terminated, the product was allowed to cool to room temperature, the resulting dark black powders were rinsed and washed with deionized water and absolute ethanol several times until free from impurities. The precipitates were dried at 75 °C in a vacuum oven for 10 h to get the sample of Ru0.63Co0.37Al2O3, Ru0.93Ni0.07Al2O3 and Ru0.54Cu0.46Al2O3 nanoparticles could be obtained. The Ru0.63Co0.37Al2O3, Ru0.93Ni0.07Al2O3 and Ru0.54Cu0.46Al2O3 nanoparticles have been characterized with the SEM, EDX, XRD analyses and FT-IR technique.

The FT-IR, SEM, EDX and XRD of NPs are shown in Fig.1, 2, 3 and 4, respectively.

4. RESULTS AND DISCUSSION

4.1. Characterization

All the synthesis processes were performed on a programmed microwave synthesis reactor (MILESTONE Marker, STARTSYNTH Microwave Synthesis Labstation Model). We used same method and technical microwave heating for solution in 600 W, 200 ˚C at 1h, but changed chemical substances, which is equipped with 50 mL quartz tube with medium stirring. The Fourier Transform Infrared spectra (FT-IR) of the samples were recorded using a Perkin Elmer Marker, Spectrum 400 Model, FT-IR spectrometer scan (4000-400cm^{-1}). NPs structures were analyzed by X-ray Diffraction (XRD, X-pert pro PANALITICAL) using the Cu-Kα radiation with 0.154 nm wavelength at 2θ angle range from 10 to 70 at 40 Kv and 30 mA. The morphologies of the samples were observed by Scanning Electron Microscopy (SEM), using a Scanning electron microscopy (SEM) and Energy Dispersive X-Ray spectroscopy (EDX) employing an accelerating voltage of 15 Kv, same machine but different result characterizations (ZEISS Marker and EVO/LS10 Model).

4.2. FT-IR analysis of $Ru_xM_{1-x}Al_2O_3$ NPs

FT-IR spectra of nanoparticles were identified and expressed in the range 400–4000 cm^{-1} wave numbers. The peaks, observed at arround 3300 cm^{-1} and between 1617-1600 cm^{-1} can be attributed to the stretching vibrations of hydrogen-bonded surface water molecules and the free hydroxyl (-OH) groups of water molecules from ambient atmosphere, respectively [16]. The absorption bands arround 2076 cm^{-1} and 1167 cm^{-1} are related to the stretching vibration of thiocarbonyl (C=S) and ethylene glycol (C–O) groups of the residual organic fuel and reducing agent. The spectra of all nanoparticles showed the peak arround 1410 cm^{-1} which is assigned to the Al-O stretching vibrations [17]. At this reaction temperature 200°C, only two characteristic strong bands of the $Ru_xM_{1-x}Al_2O_3$ structure at arround 600 and 420 cm^{-1} are observed, confirming that the complexes were decomposed completely to $Ru_xM_{1-x}Al_2O_3$ phase. These intense and weak absorption band are visible at 400–1062 cm^{-1} range are associated with the bending and stretching modes of the M-O and the M-O-M bonds corresponding to the formation of $Ru_xM_{1-x}Al_2O_3$ nanostructures [18, 19, 20, 21]. All peaks are identified and their positions are marked in the Fig. 1. These peaks correspond quite well to the reported for crystalline $Ru_xM_{1-x}Al_2O_3$ nanostructures [22].

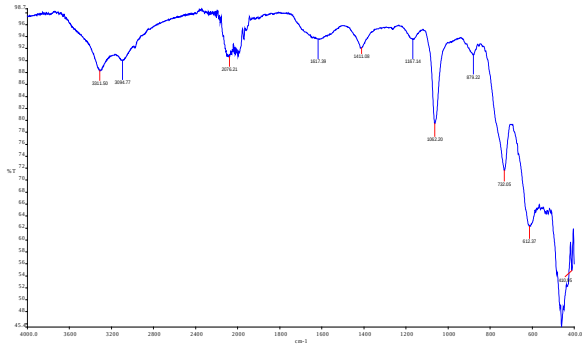

(a) $Ru_{0.4}Fe_{0.6}Al_2O_3$

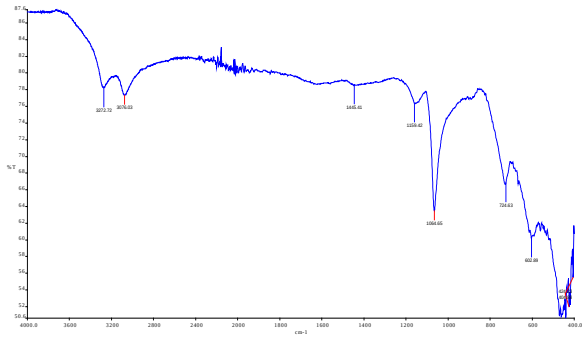

(b) $Ru_{0.63}Co_{0.37}Al_2O_3$

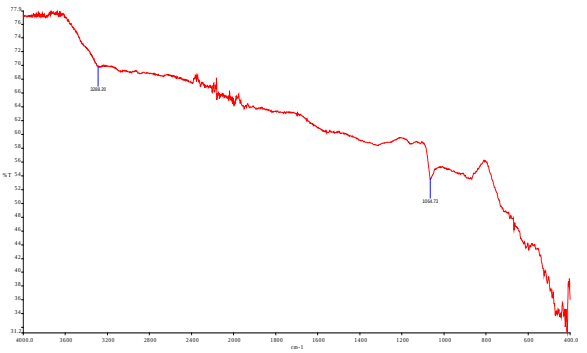

(c) $Ru_{0.54}Cu_{0.46}Al_2O_3$

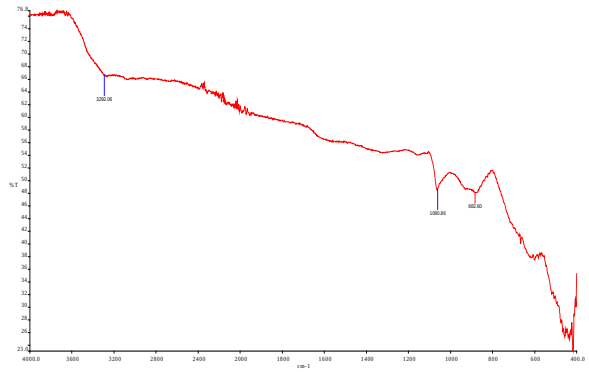

(d) $Ru_{0.93}Ni_{0.07}Al_2O_3$

Fig.1. The FT-IR spectra of RuxM1-xAl2O3 NPs

4.3. SEM analysis of $Ru_xM_{1-x}Al_2O_3$ NPs

The surface morphology of $Ru_xM_{1-x}Al_2O_3$ was investigated by the Scanning Electron Microscopy images SEM as shown in Figure 2 a,b,c,d. From the images, Figures show the formation of nanoparticles metal oxides. It can be observed from Fig.2 (a) ($Ru_{0.4}Fe_{0.6}Al_2O_3$) that the structure is actually composed of numerous nanospehere that are intercrossed with each other to form amorphous like structure. From the SEM results, the prepared crystallites are nearly spherical in shape and it can be seen that the particles congregate together and the size of which is less than 100 nm. This is probably due to the polarization of the molecules under the rapidly changing electro-magnetic field of the microwave reactor, which may result in transient, localized high temperatures for the reaction system, leading to fast synthesis with desired morphology. Real particle size can not be measured because of amorphes structure. It is a well-known fact that the temperature and reaction time are the two important factors in determining the morphology of the nanomaterials. In the conventional method, the reaction time is kept as 3 h, at 400 °C, which resulted in the formation of nanoparticles. But in microwave method, because of rapid heating, which is achieved within the few minutes, due to the suppressed diffusion process, the nano-amorphous would have been formed. The morphology is irregular and the product is amorphous phase [23]. It can be observed from Figure 2 b,c and d that the structure is amorphous like structure. The morphologies of the final products are characterized by SEM that is a typical low-magnification SEM image of $Ru_{0.63}Co_{0.37}Al_2O_3$, $Ru_{0.93}Ni_{0.07}Al_2O_3$ and $Ru_{0.54}Cu_{0.46}Al_2O_3$ nanoparticles, which is composed of many uniform flower-like microstructures with a diameter of ca. 5 nm. The high-magnification SEM image Figure 2 b,c,d reveals that the flower-like microstructure is built from many thin sheets with a thickness about 10 nm. These nanoflakes are intercrossed each other and aggregated together to form flower-like microstructures. At 200 °C, the novel $Ru_{0.63}Co_{0.37}Al_2O_3$, $Ru_{0.93}Ni_{0.07}Al_2O_3$ and $Ru_{0.54}Cu_{0.46}Al_2O_3$ nanoparticles flower-like microstructures and nanoparticles were harvested as Fig. 2b,c,d [24].

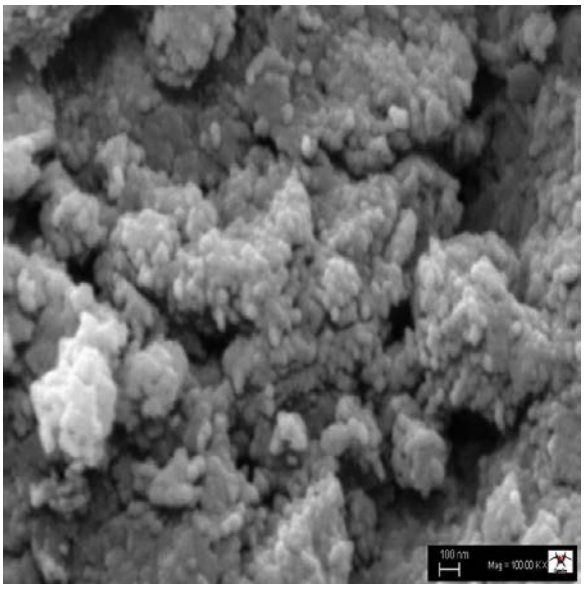

(a) $Ru_{0.4}Fe_{0.6}Al_2O_3$

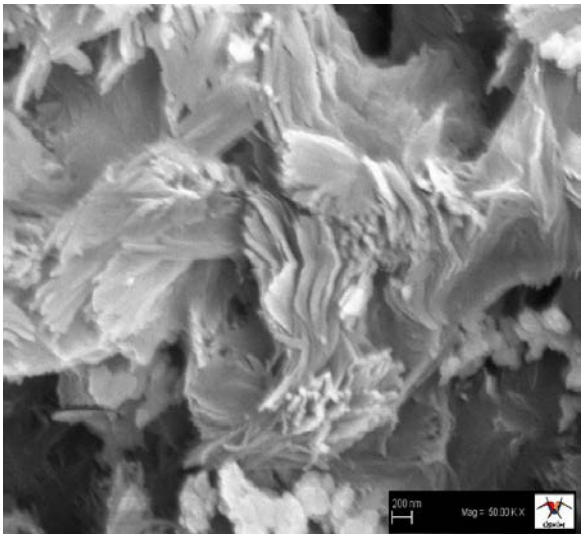

(b) $Ru_{0.63}Co_{0.37}Al_2O_3$

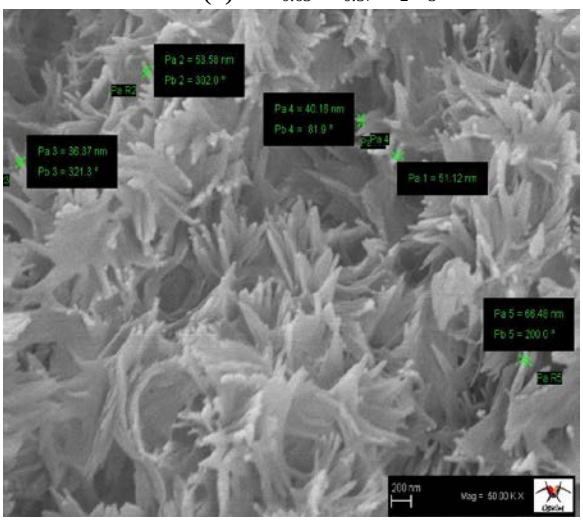

(c) $Ru_{0.93}Ni_{0.07}Al_2O_3$

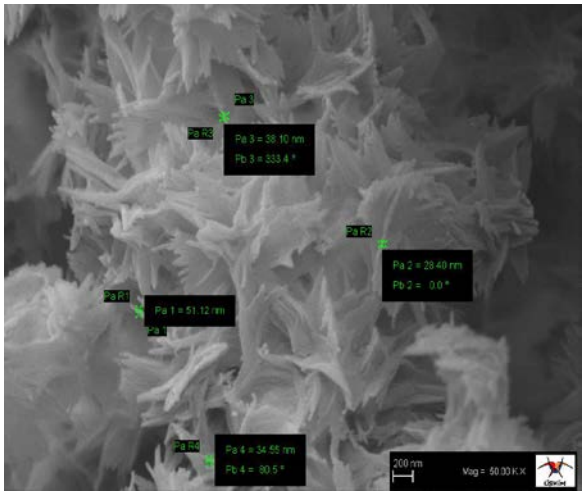

(d) $Ru_{0.54}Cu_{0.46}Al_2O_3$

Fig. 2. SEM images of the $Ru_xM_{1-x}Al_2O_3$ NPs

4.4. EDX analysis of the $Ru_xM_{1-x}Al_2O_3$ NPs

EDX, Energy dispersive X-ray spectroscopy (Fig.3) illustrated the chemical nature of synthesized $Ru_xM_{1-x}Al_2O_3$ NPs. The peak obtained at the energy of 2.6 keV for Ru and also some weak peaks for O, Al, M (Co,Ni and Cu) and Au have also been found. The atomic percentages of Al and O were found to be ca 40 % and 60 %, respectively. The atomic ratio of Al and O is 2:3, which approaches the theoretical value for Al_2O_3. This observation further confirms that the final product is only highly pure $Ru_xM_{1-x}Al_2O_3$ type NPs [18]. The EDX results showed the presence of $Ru_{0.4}Fe_{0.6}Al_2O_3$, $Ru_{0.63}Co_{0.37}Al_2O_3$, $Ru_{0.93}Ni_{0.07}Al_2O_3$ and $Ru_{0.54}Cu_{0.46}Al_2O_3$ by the appearance of Fe, Co, Ni and Cu peaks in the spectrum, respectively. The absence of carbon, nitrogen and other impurities are also evidenced from the EDX spectrum. This analysis confirmed that the sample $Ru_xM_{1-x}Al_2O_3$ type NPs prepared by microwave-assisted method. Hence, the result is definitive evidence to suggest that the sample does not contain any other element and are indeed free from other impurities. The peaks at 2.1–2.2 keV in the EDX spectra are due to the gold, which is coated on the samples before recording SEM [25].

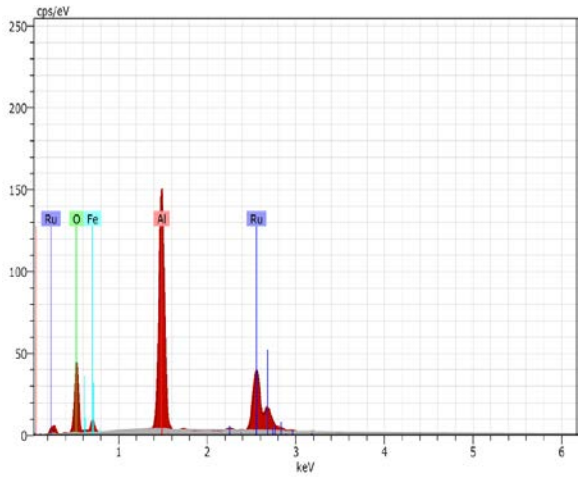

(a) $Ru_{0.4}Fe_{0.6}Al_2O_3$

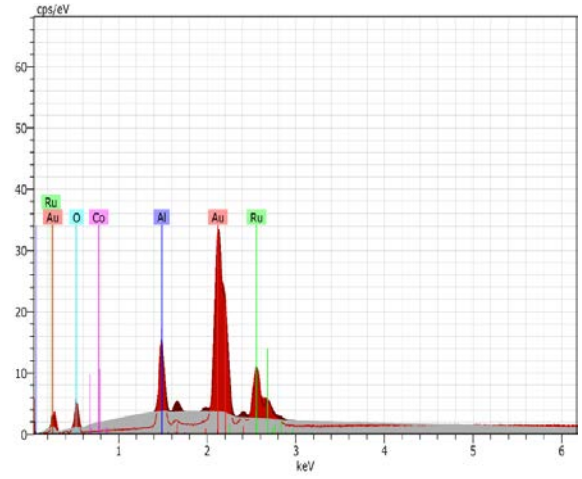

(b) $Ru_{0.63}Co_{0.37}Al_2O_3$

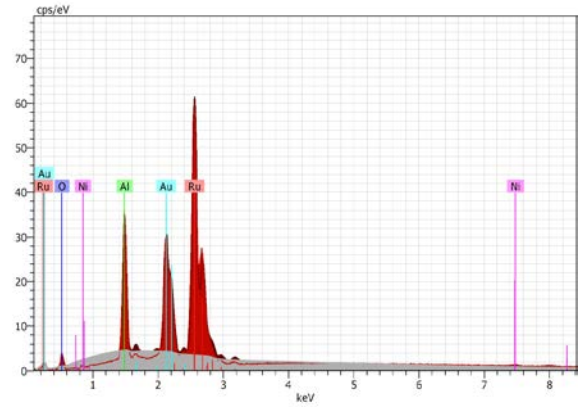

(c) $Ru_{0.93}Ni_{0.07}Al_2O_3$

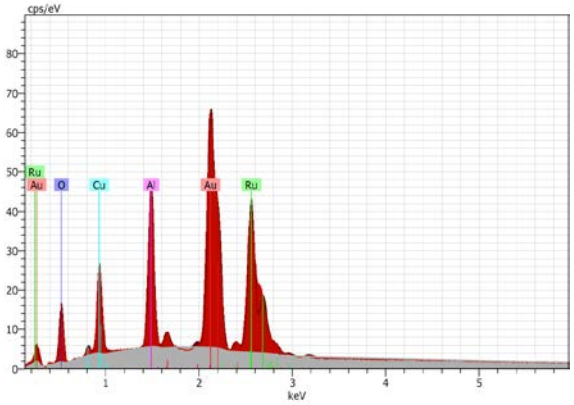

(d) $Ru_{0.54}Cu_{0.46}Al_2O_3$

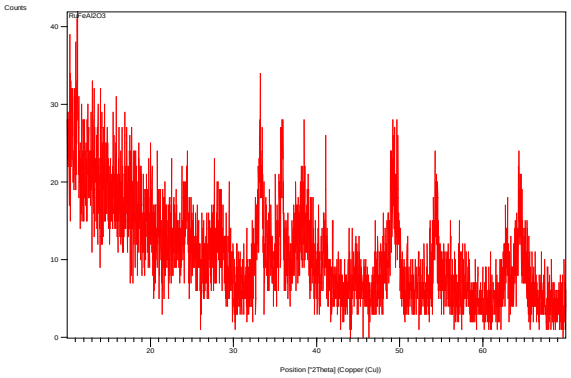

(a) $Ru_{0.4}Fe_{0.6}Al_2O_3$

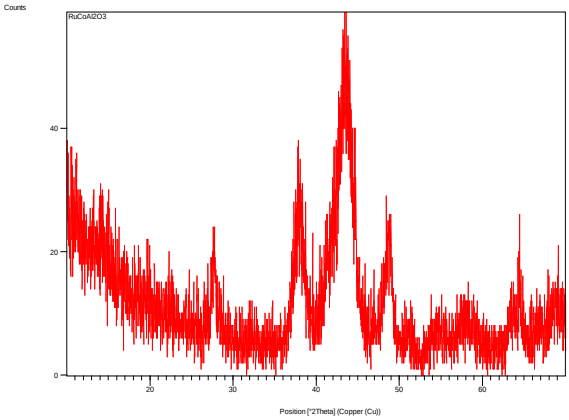

(b) $Ru_{0.63}Co_{0.37}Al_2O_3$

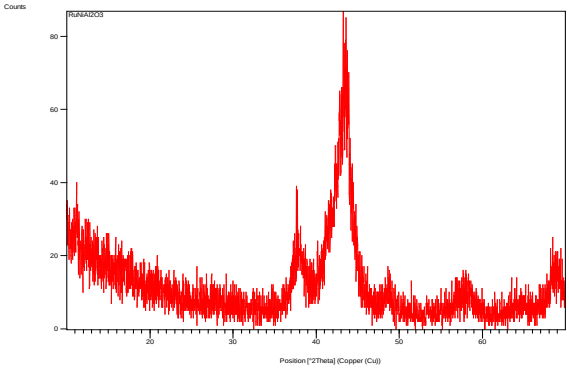

(c) $Ru_{0.93}Ni_{0.07}Al_2O_3$

Fig. 3. EDX of the $Ru_xM_{1-x}Al_2O_3$ NPs

4.5. XRD analysis of $Ru_xM_{1-x}Al_2O_3$ NPs

The XRD establishes the phase purity and crystallinity, confirm the product formation [26], is shown in Fig. 4 that presents the XRD patterns of the decomposition products of the complexes at 200 °C. With the increase in temperature and stirring, metal ions are complexed with thiourea and form metalthiourea complexes. Well-defined diffraction peaks at about 24°, 28°, 33°, 38°, 45°, 54° and 65° are observed for $Ru_{0.4}Fe_{0.6}Al_2O_3$, corresponding to the crystals. This result confirms that the complex was decomposed completely into the $Ru_{0.4}Fe_{0.6}Al_2O_3$, phase at 200°C, in good agreement with FT-IR results. Some impurity peaks were found in the XRD patterns, confirming that the product is not well crystallized with high purity. As can be seen, the diffraction peaks are broadened because of the small size effect of the nanoparticles. The average crystallite size (d) was calculated to be less than 100 nm by the Scherrer relation $d = 0.9\lambda/(B\cos\theta)$, where λ is the wavelength of Cu Kα radiation, B is the corrected full width at half maximum of the diffraction peak, and θ is the Bragg angle. As shown in Fig. 4, new phase was observed when the metal changed. The ununiform $Ru_{0.4}Fe_{0.6}Al_2O_3$ particles have sphere-like shapes with agglomeration. And another $Ru_{0.63}Co_{0.37}Al_2O_3$, $Ru_{0.93}Ni_{0.07}Al_2O_3$ and $Ru_{0.54}Cu_{0.46}Al_2O_3$ NPs have flower-like shapes with weak agglomeration [18]. The diffraction peaks at about 28°, 37°, 43°, 48°, 54°, 58°, 64° and 69° for $Ru_{0.63}Co_{0.37}Al_2O_3$, peaks at about 38°, 48°, 58°, 65° and 68° for $Ru_{0.93}Ni_{0.07}Al_2O_3$ and at about 38°, 43°, 48° and 58° for $Ru_{0.54}Cu_{0.46}Al_2O_3$ nanoparticles, are observed. These XRD pattern clearly showed that the sythesized nanoparticles formed by three metals are crystalline in nature.

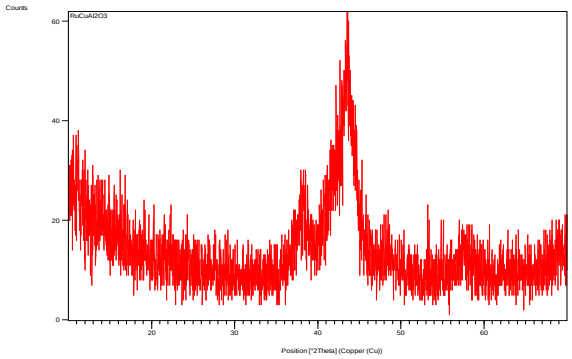

(d) $Ru_{0.54}Cu_{0.46}Al_2O_3$

Fig. 4. XRD spectra of the $Ru_xM_{1-x}Al_2O_3$ NPs

5. CONCLUSIONS

$Ru_xM_{1-x}Al_2O_3$ (M: Fe, Co, Ni and Cu) type nanoparticles were successfully prepared by a controlled microwave–assisted co-precipitation. According to the results, the microwave co-precipitation inclined to form homogeneous and irregular shape particles which are less than 100 nm in size. The EDX analysis confirmed that the prepared material has a high purity and the presence of elements like Fe, Co, Ni and Cu in trace level. FT-IR study confirms the presence of metal-oxygen and metal-oxygen-metal bond. We propose this synthesis method that is rapid, facile, convenient, less time consuming and environmentally safe, to be used for metal oxide nanoparticles.

6. ACKNOWLEDGEMENTS

This work is financially supported by the Kahramanmaraş Sütçü İmam University, Graduate School of Natural and Applied Sciences, BAP, Project no: 2013/4-14, authors gratefully thank USKIM for SEM, EDX and XRD facilities.

7. REFERENCES

[1] Krishnakumar T., Jayaprakash R., Pinna N., Singh V.N., Mehta B.R., Phani A.R., (2009), “Microwave-assisted synthesis and characterization of flower shaped zinc oxide nanostructures”, Mater. Lett. 63, 242.

[2] UmaSangari N., ChitraDevi S., (2013), “Synthesis and characterization of nano ZnO rods via microwave assisted chemical precipitation method”, J. Solid State Chem., 197, 483.

[3] Shen Y., Li W., Li T., (2011), “Microwave-assisted synthesis of BaWO4 nanoparticles and its photoluminescence properties”, Mater. Lett. 65, 2956.

[4] Astruc D., (2008), “Nanoparticles and Catalysis”, Wiley-VCH Verlag GmbH & Co. KGaA, Weinheim, 349.

[5] Ranu B.C., Chattopadhyay K., Adak L., Saha A., Bhadra S., Dey R., Saha D., (2009), “Metal nanoparticles as efficient catalysts for organic reactions”, Pure Appl. Chem. 81, 2337.

[6] Jia J. C., Schüth F., (2011), “Colloidal metal nanoparticles as a component of designed catalyst” Phys. Chem. 13, 2457.

[7] Li Y., Somorjai G.A., (2010), “Nanoscale advances in catalysis and energy applications”, Nano Lett. 10, 2289.

[8] Joo S.H., Park J.Y., Renzas J.R., Butcher D.R., Huang W., Somorjai G.A., (2010), “Size effect of ruthenium nanoparticles in catalytic carbon monoxide oxidation”, Nano letters 10, 2709.

[9] Su F., Lee F.Y., Lv L., Liu J., Tian X.N., Zhao X.S., (2007), “Sandwiched ruthernium/carbon nanostructures for highly active heterogeneous hydrogenation”, Adv. Funct. Mater. 17, 1926.

[10] Liu H., Song C., Zhang L. , Zhang J., Wang H., Wilkinson D.P., (2006), “A review of anode catalysis in the direct methanol fuel cell”, J. Power Sources, 155, 95.

[11] Kang J., Zhang S., Zhang Q., Wang Y., (2009), “Ruthenium Nanoparticles Supported on Carbon Nanotubes as Efficient Catalysts for Selective Conversion of Synthesis Gas to Diesel Fuel” Angew. Chem. 121 2603.

[12] Perkas N., Minh D.P., Gallezot P., Gedanken A., Besson M., (2005), “Antibacterial activity of Ruthenium Nanoparticles synthesized using Gloriosa superba L. Leaf extract” Appl. Catal. B:Environ. 59 121.

[13] Algul O., Kaessler A., Apcin Y. , Yilmaz A., Jose J., (2008) “Comparative Studies on Conventional and Microwave Synthesis of Some Benzimidazole, Benzothiazole and Indole Derivatives and Testing on Inhibition of Hyaluronidase”, Molecules, 13, 736.

[14] Glaspell G., Fuoco L., El-Shall M.S., (2005), “Microwave synthesis of supported Au and Pd nanoparticle catalysts for CO oxidation”, J. Phys. Chem. B 109, 17350.

[15] Gupta S., Giordano C., Gradzielski M., Mehta K. S., (2013) , "Microwave-assisted synthesis of small Ru nanoparticles and their rolein degradation of congo red", J. Coll. Inter. Sci., 411, 173.

[16] Wang, Z., Xie Y., Wangb, P., Mab, Y., Jin, S., Liu, X., (2011), "Micro wave anneal effect on magnetic properties of Ni0.6Zn0.4Fe2O4 nano-particles prepared by conventional hydrothermal method", J. Magn.Mag. Mater., 323, 3121.

[17] Krishnakumar T., Jayaprakash R., Pinna V.N., Singh B.R., Mehta A.R., (2009), "Microwave-assisted synthesis and characterization of flower shaped zinc oxide Nanostructures", Mater. Letters, 63, 242.

[18] Farhadi S., Pourzare K., Sadeghinejad S., (2013), "Simple preparation of ferromagnetic Co_3O_4 nanoparticles by thermal dissociation of the $[Co^{II}(NH_3)_6](NO_3)_2$ complex at low temperature", J. Nanostruc.Chem., 3, 16.

[19] Souza A. E., Santos G.T. A., Silva R.A., (2012), "Morphological and Structural changes of $Ca_xSr_{1-x}TiO_3$ Powders Obtained by the Microwave-Assisted Hydrothermal Method", J. Appl. Ceram. Technol., 9, 186.

[20] Santos, T., Valente, M. A., Monteiro, J., Sousa, J., Costa, L. C. (2011), "Electromagnetic and thermal history during microwave heating", Appl.Therm. Engin., 31, 3255.

[21] Krishnakumar, T., Jayaprakash, R., Pinna, N., Singh, V. N., Mehta, B. R., Phani, A. R. (2009), "Microwave-assisted synthesis and characterization of flower shaped zinc oxide nanostructures" Materials Letters, 63, 242

[22] UmaSangari N., ChitraDevi S., (2013), "Synthesis and characterization of nano ZnO rods via microwave assisted chemical precipitation method" J. Solid State Chem. 197, 483.

[23] Ragupathi, C., Kennedy, L. J., Vijaya, J. J., (2014), "A new approach: Synthesis, characterization and optical studies of nano-zinc aluminate" Adv. Powder Tech., 25, 267.

[24] Li Z.Q., Chen X.T., Xue Z.L, (2013), "Microwave-assisted synthesis and photocatalytic properties of flower-like Bi2WO6 and Bi2O3–Bi2WO6 composite", J. Coll.Inter.Sci., 394, 69

[25] Azam A., (2012), "Microwave assisted synthesis and characterization of Co doped Cu ferrite nanoparticles", J. Alloys Comp., 540, 145

[26] UmaSangari N., ChitraDevi S., (2013), "Synthesis and characterization of nano ZnO rods via microwave assisted chemical precipitation method", J. Solid State Chem., 197, 483.

[27] Kawasaki H., (2013), "Surfactant-free solution-based synthesis of metallic nanoparticles toward efficient use of the nanoparticles ' surfaces and their application in catalysis and chemo-/biosensing", Nanotech. Rev, 2,